

Optical Consequences of Slushcast Components

P. Skensved, B. C. Robertson, W. Frati and M. M. Lowry
SNO-STR-92-014

March 18, 1992

Introduction

There are significant financial advantages to using slushcast for the acrylic neck and for the collar that fits the neck tube to the top of the acrylic sphere. The radioactivity of slushcast is of the order of 10 ppt and a slushcast neck would contribute a neutron background that is only 1% of that from the acrylic sphere at White Book levels. Similarly a slushcast collar would contribute about 3% of that from the acrylic sphere.

The outstanding question to be answered is whether the optical consequences of using slushcast are acceptable from the physics point of view. All that is known at present is that one sample (aged) has been measured at Chalk River and was found to be essentially black for the relevant thickness and frequency range. Accordingly, in the following it will be assumed that all slushcast components are black.

All previous modelling of the detector has taken no recognizance of the neck; *i.e.* phototube cover right over the top of the detector and uniform

2" acrylic thickness. Therefore we do not have a full realistic reference calculation for comparison.

Effect of Neck Hole

In order to estimate the importance of the loss of light collection due to the loss of approximately 19 phototubes because of the presence of the neck, a comparison of the detector response to 10.5 MeV electron sources was done with and without the top 19 phototubes removed. These are shown in Figs. 1 and 2 for a source uniformly distributed about the detector volume. No difference is observed. (Both spectra show a non-statistical broadening due to the reduction of phototube hits for events where the light is attenuated by passing through a large amount of water compared to events where the light shines into nearby phototubes.) A more sensitive comparison is found in Figs. 3 and 4, where a point source into 4π was placed at a radius of 5.5 meters directly under the centre of the neck, and in Figs. 5 and 6, where a point source was placed at the same radius but approximately 75 cm off axis. Neither case shows an observable difference due to the removal of the 19 PMTs.

Slushcast Neck Calculations

The calculation done using a 10.5 MeV electron source uniformly and isotropically distributed throughout the detector volume (Fig. 2) was repeated with a black acrylic neck, corresponding to the situation expected for a slushcast neck. The results are shown in Fig. 7. No difference is observed within the resolution of the peak. This indicates that there is no major effect due to light loss from a black neck.

In order to understand better the effect of the neck an analytic estimate was done by assuming that the effect of the black neck was to create a shadow zone where there is a reduced efficiency for detecting photons. For simplicity this zone was taken to be black. The extent of the zone was estimated in two cases, one an extreme situation and one an average. For the extreme case it was fixed by using the shadow cast by the neck for an event on the vertical axis of the detector at a radius of 5.5 m. In this case

the disk was found to cover a region having a zenith angle from the detector centre down 20° vertically, *i.e.* a diameter of about 6 meters. This is most appropriate for events near the neck, and seriously overestimates the light loss for events further away from the neck. For the average situation the effect was estimated by using the neck diameter to cast a shadow for events started from the waist of the vessel. This results in a darkened arc length of about 2 meters. The geometries of these two conditions are indicated in Fig. 8.

The effect of blocked light is to reduce the number of hit phototubes in an event which shines in the direction of the disk. The magnitude of the energy shift for such an event was determined by the intersection of the Cherenkov ring with the shadow zone. This was estimated simply by taking the ratio of the disk's diameter (6 m in the extreme case) or arc length (2 m in the average case) to the circumference of a cone with an opening angle of 45° . This assumes that most rings cross the disk close to the centre and from a distance large compared to the ring's radius. This is a significant underestimate for events near the top heading into the neck.

The fraction of events affected by the neck for any given source position was estimated using the solid angle covered by the disk for a point on the vertical axis at the same height as the source location. The active volume of the detector was approximated by a uniform shell at a radius of 5.5 metres. Using these approximations the fractional light loss and relative probability of intersecting the disk was calculated as a function of zenith angle. In this way it was estimated that 95% to 99% of the events were unaffected by the disk and that in the 95% case the remaining 5% of the events were shifted down in energy approximately uniformly to about 75% of the full energy peak with a broad maximum at about 90% of the full energy peak. This case is shown in Fig. 9. It is interesting to note that for the case where the area covered by the disk was about 3% of the full PMT sphere, the fraction affected by the disk in the above calculation was $100\% - 95\% = 5\%$.

Slushcast Collar Calculations

Calculations have been done for the collar in a similar way to the neck. The Monte Carlo results are shown for the case of combined neck and collar in

Fig. 10, and again show no significant distortion. Also the analytic estimate indicates that from 1 to 5% of the event from the whole detector would be affected by the collar and would be spread down in energy by up to about 7%.

Discussion

The analytic calculation, although admittedly very crude, indicates why it is not surprising that no effect was observed in the Monte Carlo calculation. The number of events affected is small and the shift for those events affected is on a scale comparable to the resolution available to a 10 MeV electron event.

That there is an effect, and that the Monte Carlo can see this effect, can be seen in Fig. 11, where the electron source was placed at a radius of 5.5 m directly under the black acrylic neck and allowed to shine into 4π . At this location the Cerenkov light cone closely matches the neck shadow, and a significant distortion of the energy and direction information can be seen clearly. There are two mechanisms responsible for the distortion of the detector response to the electrons. The obscuration due to the neck can cause a reduction of observed light anywhere from no loss to full loss, and so can be expected to produce a broad spectrum with a peak roughly at half of the full energy. The second effect is that the majority of those events unaffected by the collar have suffered the greatest water attenuation because they are generally pointing to the far side of the detector, shifting them down in energy as noted in Figs. 1 and 2. When the collar is present the effect is even more pronounced (Fig. 12). It should be noted that the absence of the PMTs that have to be removed for the neck insertion does not contribute significantly to this distortion (Fig. 4). A similar, although not so severe effect is seen if the source location is displaced 75 cm to the side at the 550 cm radius (Figs. 13, 6). Moving the source further away radially (Figs. 14, 15) indicate that the effect dies quickly with distance from the neck, and suggest that a volume of perhaps a few cubic meters of water next to the neck are affected. (A summary of first and second moments of the spectra is given in Table 1.)

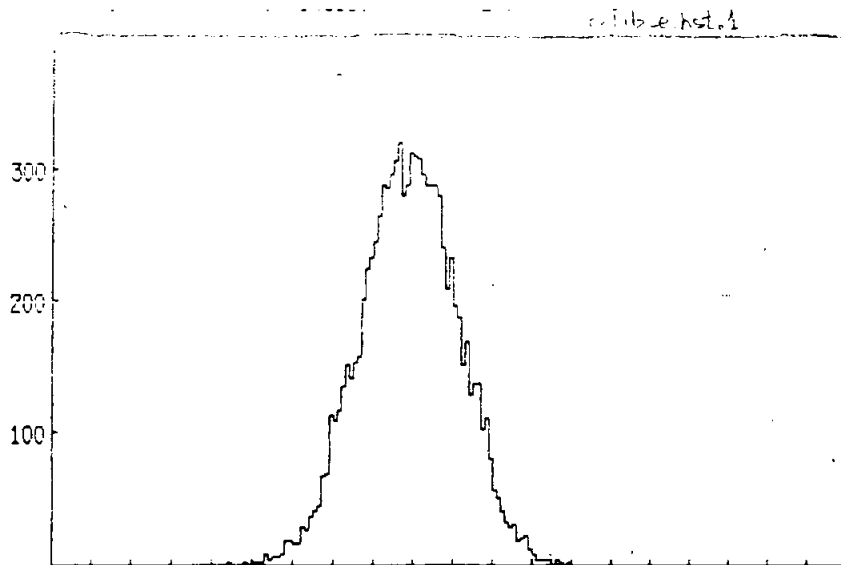
The effect of using optical quality acrylic for the neck and collar can be estimated roughly using the average transmission information in SNO-

STR-91-046 for 2 inch Rohm material and a source position at the centre of the detector. In this way an average attenuation length of 19.45 cm can be obtained. If an average light penetration angle of 45° and neck thickness of 2.5 inches is used, then a maximum of approximately 60% of the light penetrates through the neck per layer to be passed through. This indicates that the magnitude of the energy shift would be approximately *half* that of slushcast for an optical quality neck. For the collar a minimum of about 12 inches of acrylic would have to be penetrated, so that only about 20% of the light would be collected.

It appears that the major effect of using an opaque neck and collar would result in not more than about 1% of the events from the heavy water being shifted in energy by an amount greater than the intrinsic energy resolution. The major consequence of using slushcast would be the need for more careful calibration techniques in the immediate vicinity of the neck. That extra care would be required in this region was in any case true, since even optical quality acrylic in the neck and collar would significantly affect the perceived properties of events in this region.

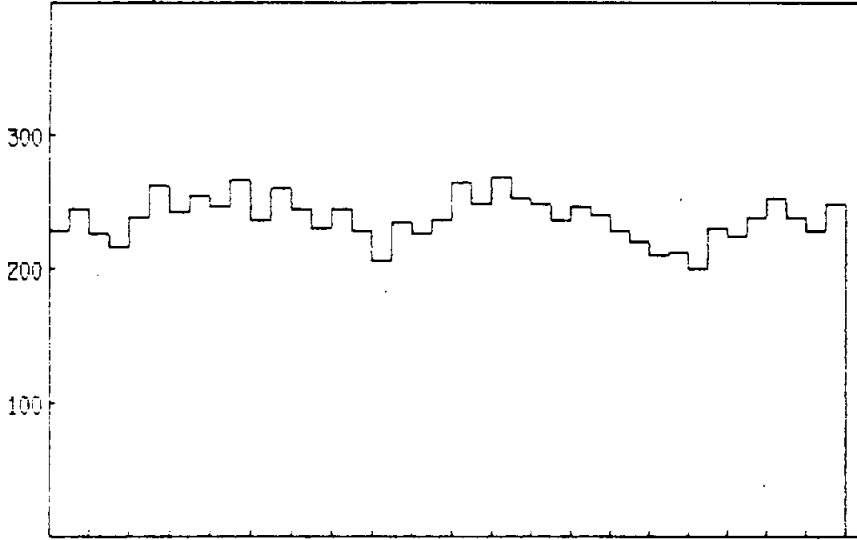
Model	Source	Events	N_{hit}	σ	Figure
standard detector	uniform D ₂ O	10,000	88.537	11.971	1
top 19 PMTs missing	uniform D ₂ O	10,000	88.610	11.973	2
standard detector	(0,0,550)	2,000	84.840	10.926	3
top 19 PMTs missing	(0,0,550)	2,000	83.896	10.453	4
standard detector	(53,53,550)	2,000	84.910	11.138	5
top 19 PMTs missing	(53,53,550)	2,000	83.576	10.341	6
black neck	uniform D ₂ O	10,000	87.872	11.988	7
black neck + collar	uniform D ₂ O	10,000	87.739	12.108	10
black neck	(0,0,550)	2,000	65.683	17.728	11
black neck + collar	(0,0,550)	2,000	59.302	20.266	12
black neck + collar	(53,53,550)	2,000	73.631	14.242	13
black neck + collar	(0,0,500)	2,000	72.896	15.253	14
black neck + collar	(0,0,450)	2,000	80.561	12.796	15

Table 1:



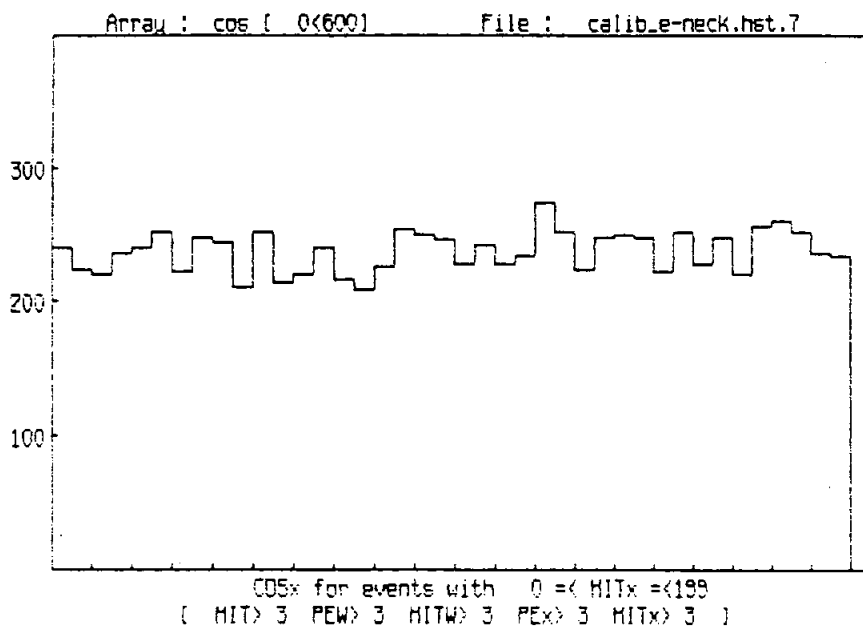
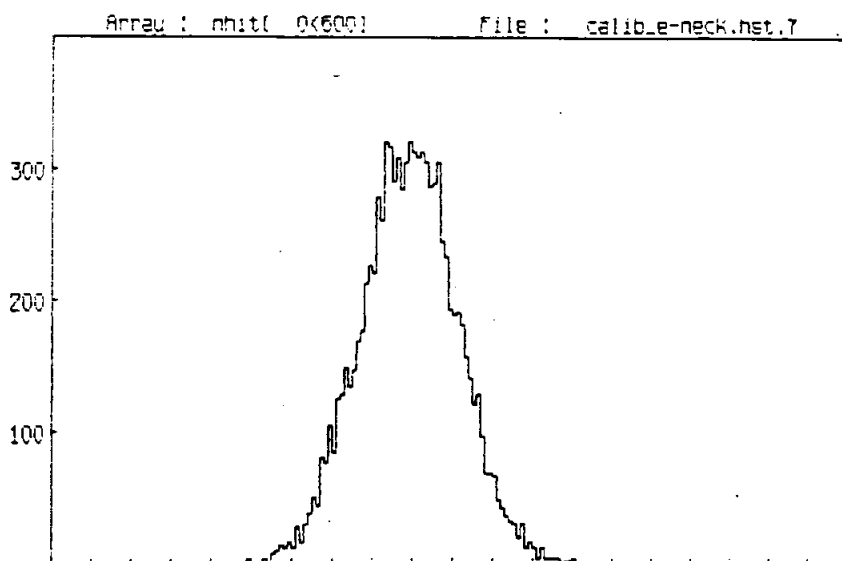
HITx for events with $0 \leq \text{COSx} \leq 40$
 (HIT> 3 PEW> 3 HITW> 3 PEX> 3 HITx> 3)

Array : cos [0<600] File : calib.e.hst.1



COSx for events with $0 \leq \text{HITx} \leq 189$
 (HIT> 3 PEW> 3 HITW> 3 PEX> 3 HITx> 3)

10000 e⁻ 10.511 MeV
 uniformity in θ_{20}
 standard detector

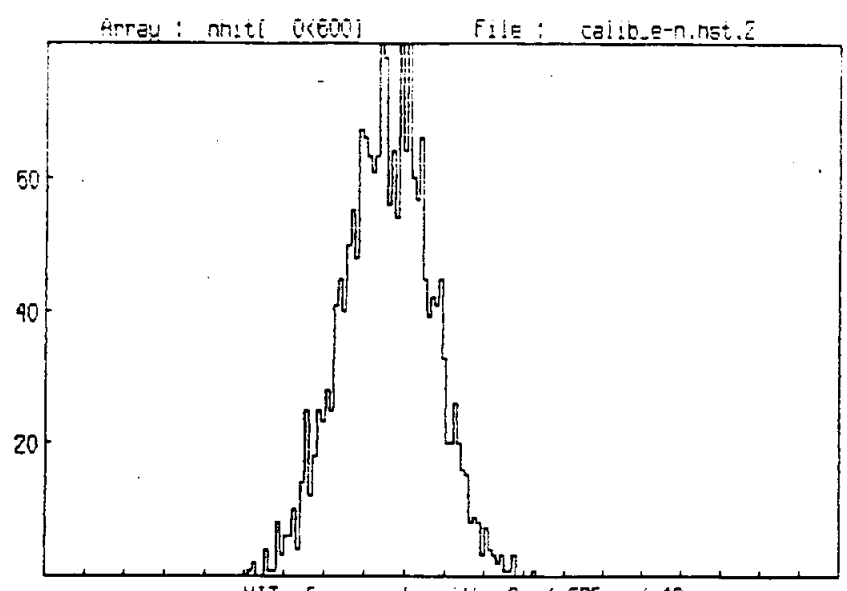


10,000 e^- 10.511 MeV

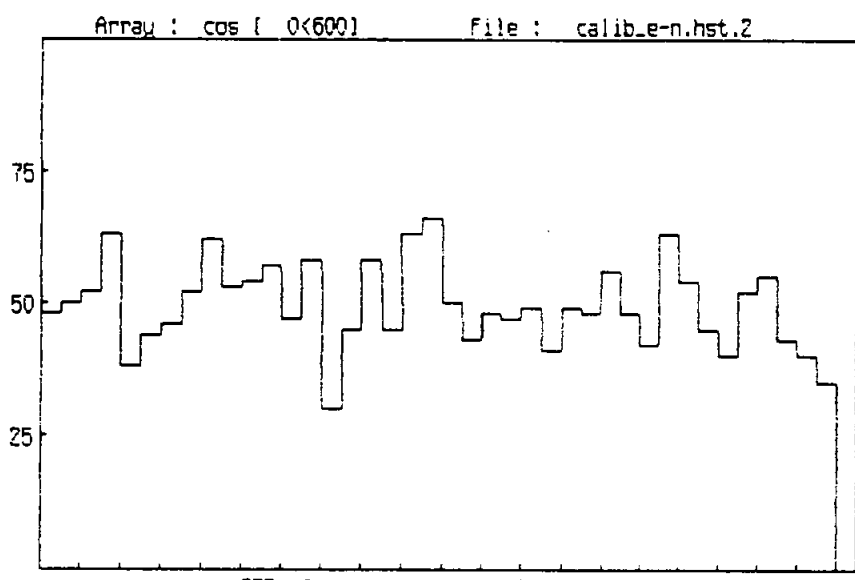
uniformly $\cos \theta_{3c}$

top 19 PMTs missing

fig 2



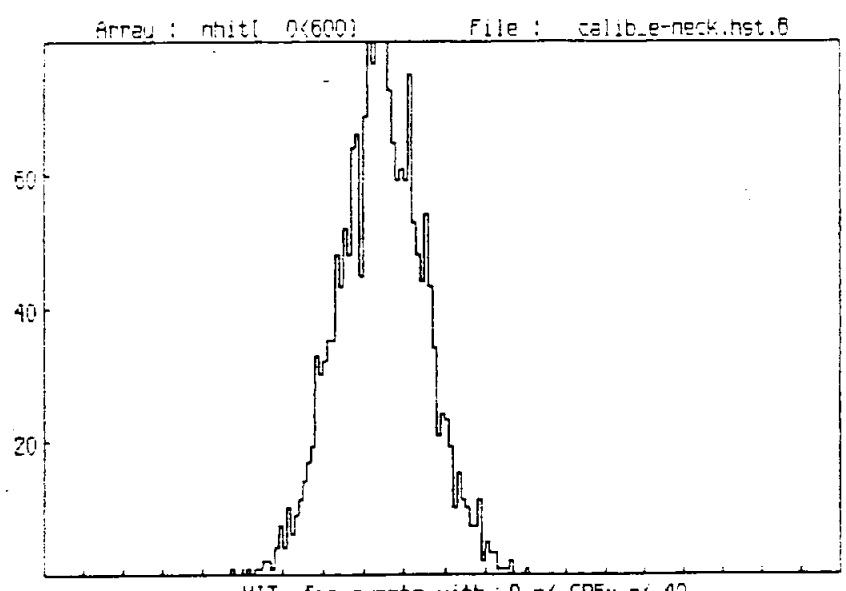
HITx for events with $0 \leq \text{COSx} \leq 40$
 [HIT> 3 PEW> 3 HITW> 3 PEX> 3 HITx> 3]



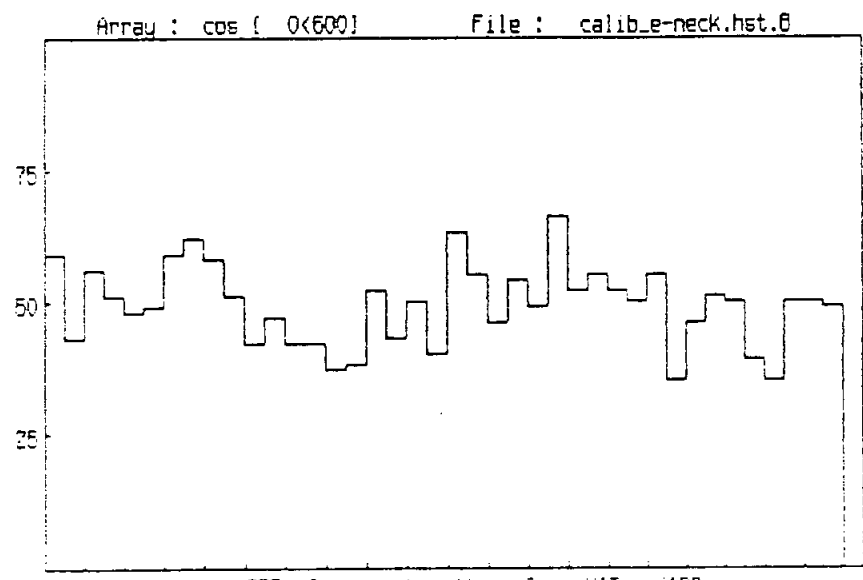
COSx for events with $0 \leq \text{HITx} \leq 199$
 [HIT> 3 PEW> 3 HITW> 3 PEX> 3 HITx> 3]

2,000 e⁻ 10.511 MeV
 (0, 0, 550)
 a few & ...
 standard detector

fig 3



HITx for events with 0 ≤ COSx ≤ 40
 (HIT > 3 PEW > 3 HITW > 3 PEX > 3 HITx > 3)

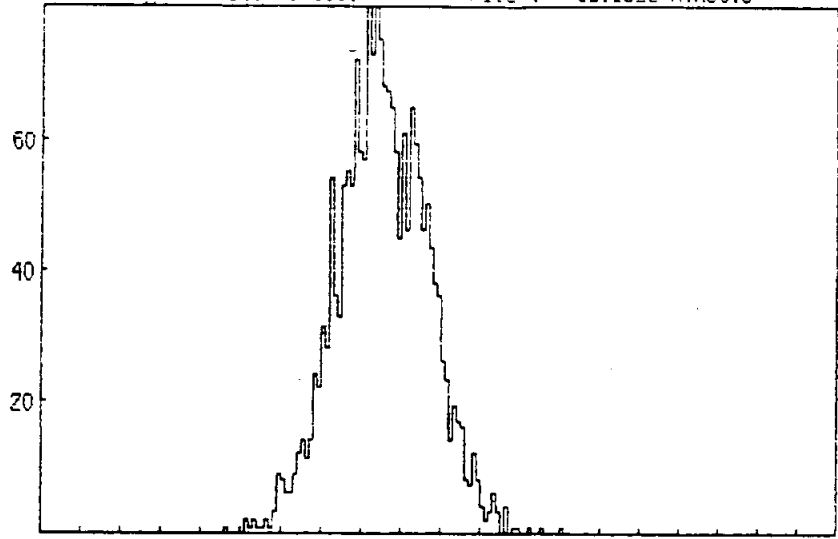


COSx for events with 0 ≤ HITx ≤ 199
 (HIT > 3)

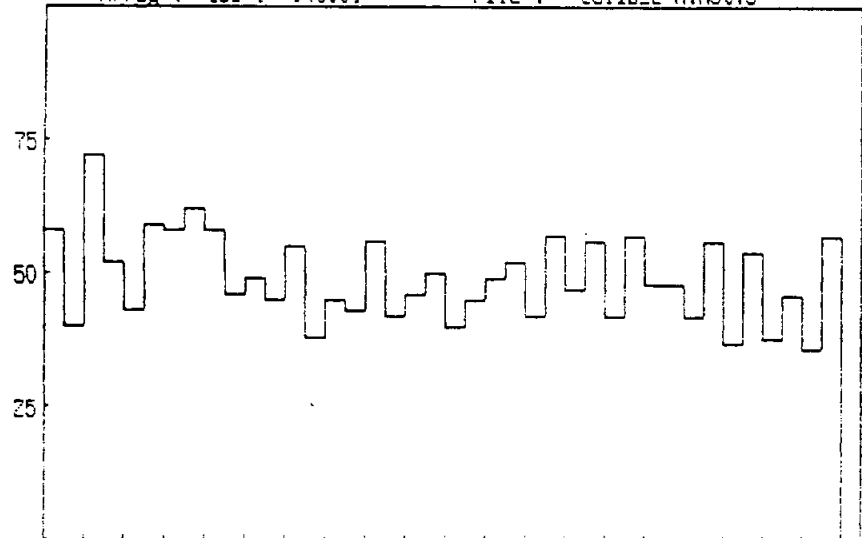
[03]

2000 e⁻ 105 100
 (0,0,550)
 top 19 PMTs missing

Array : nhit(0<600) File : calib_e-n.hist.3

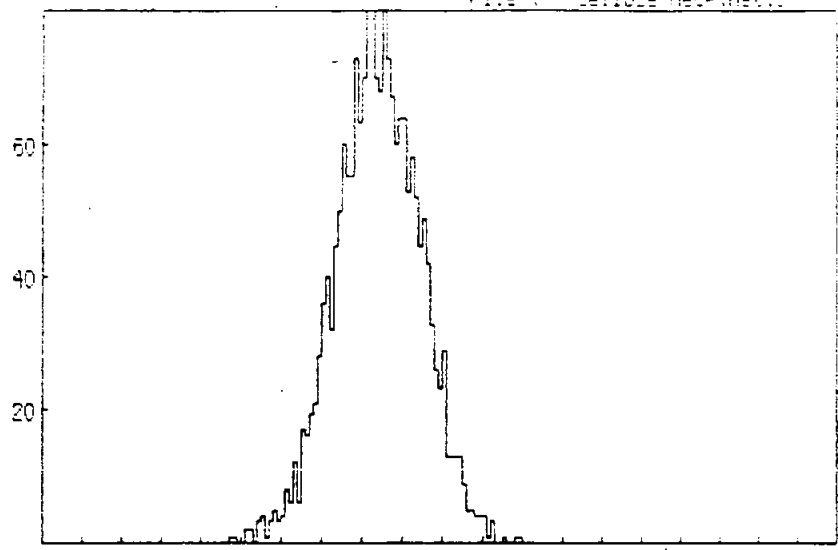


Array : cos (0<600) File : calib_e-n.hist.3



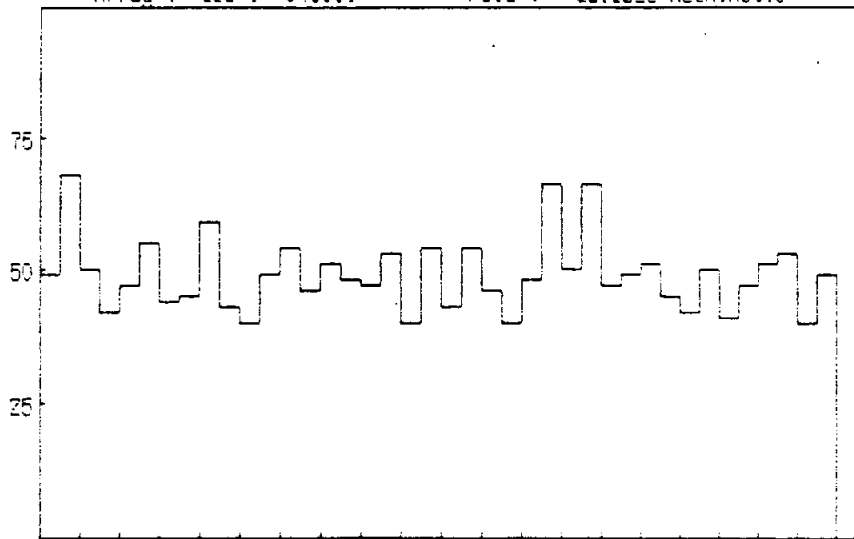
2,000 e- 10.5 MeV
 (53, 53, 550)
 standard detector

FILE : CALIB-E-NECK.DEC.3



HITx for events with 0 <= COSx <= 40
(HIT > 3 PEW > 3 HITW > 3 PEX > 3 HITx > 3)

Arrau : cos [0<600] File : calib_e-neck.hst.3

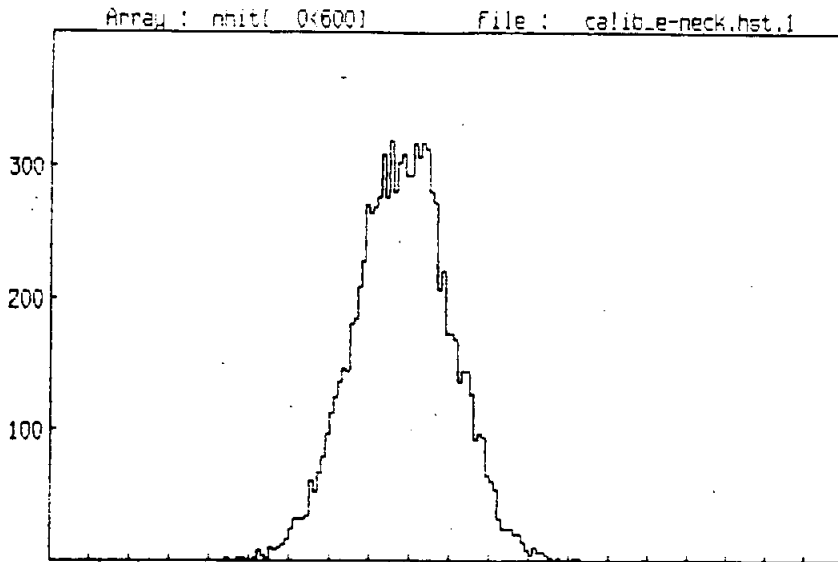


COSx for events with 0 <= HITx <= 199
(HIT > 3 PEW > 3 HITW > 3 PEX > 3 HITx > 3)

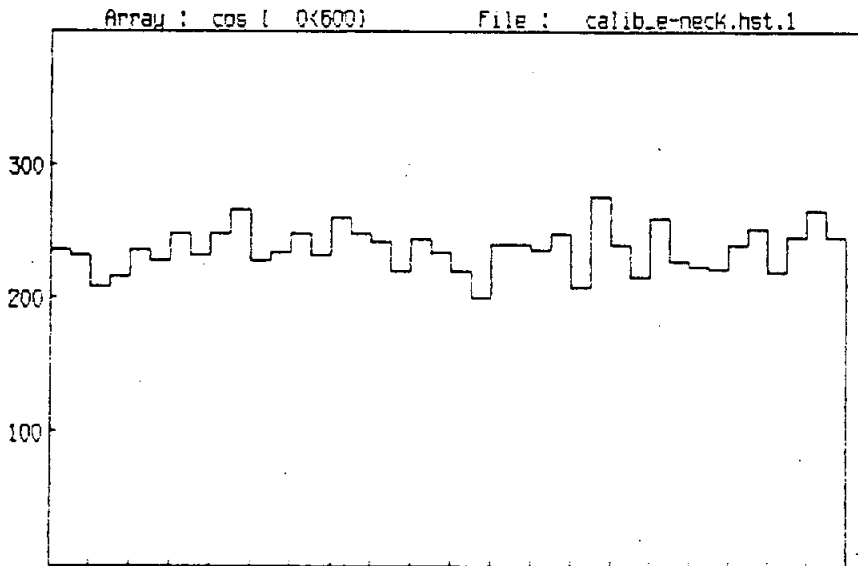
2000 e⁻ 10.5 MeV

(53, 43, ...)

top 19 PMT s missing



HITx for events with $0 \leq \text{COSx} \leq 40$
 (HIT> 3 PEW> 3 HITW> 3 PEX> 3 HITx> 3)



COSx for events with $0 \leq \text{HITx} \leq 199$
 (HIT> 3 PEW> 3 HITW> 3 PEX> 3 HITx> 3)

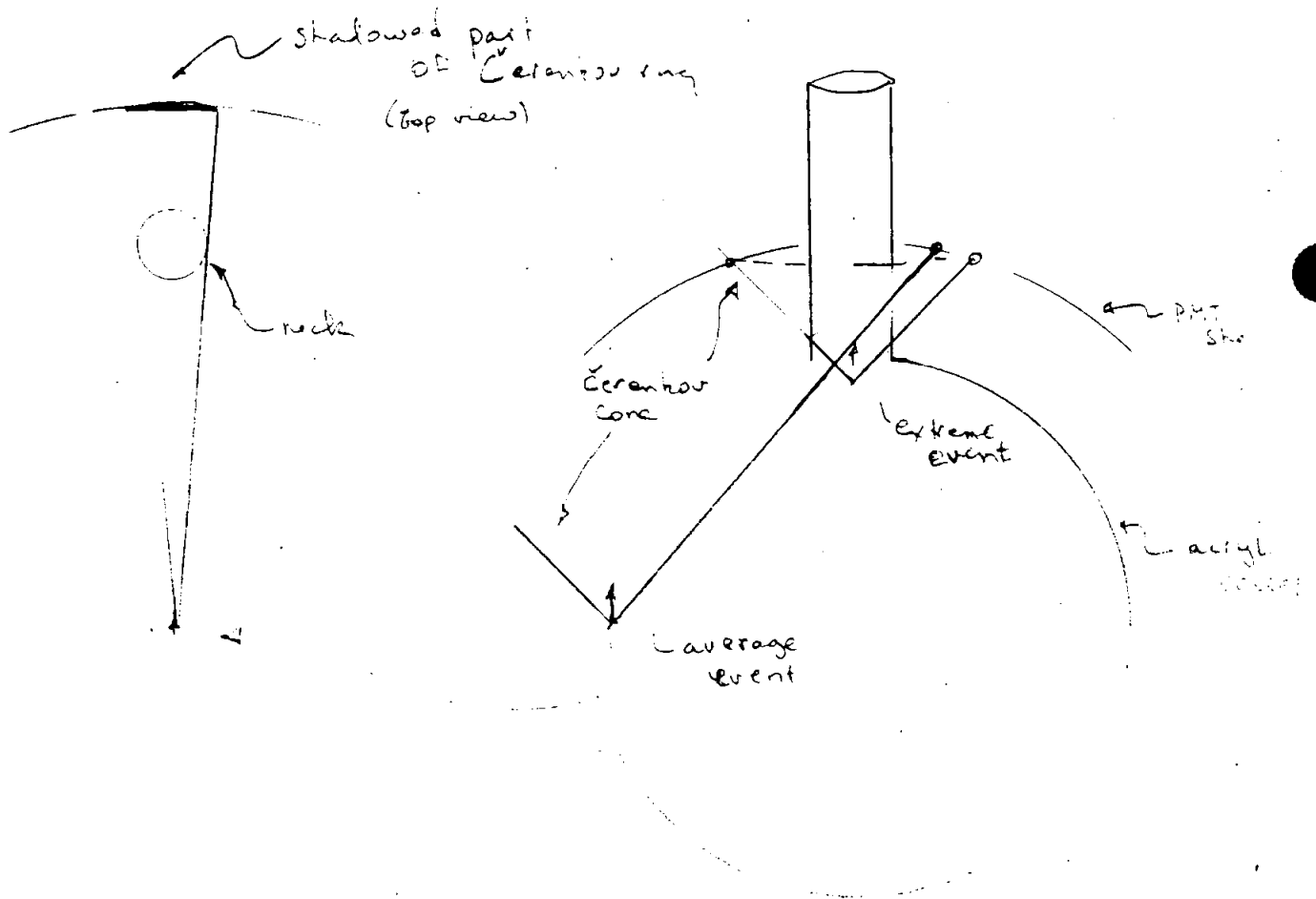
10,000 e⁻ 10.511 keV

Uniformly in D₂O

measured in a neck
 no-transparent neck

fig 7

Analytic Event Geometries



Spectral Distortion due to 6 m Disk

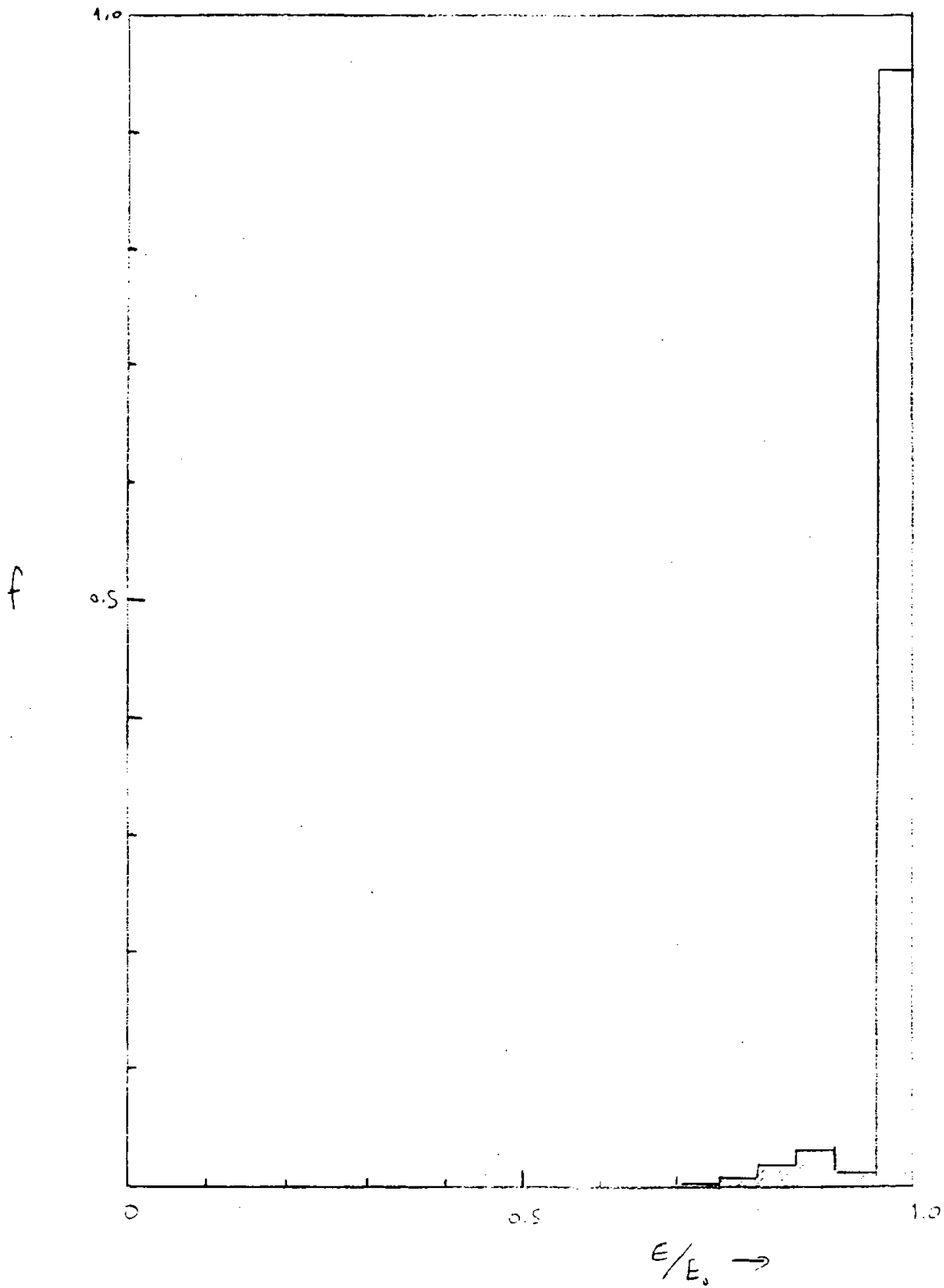
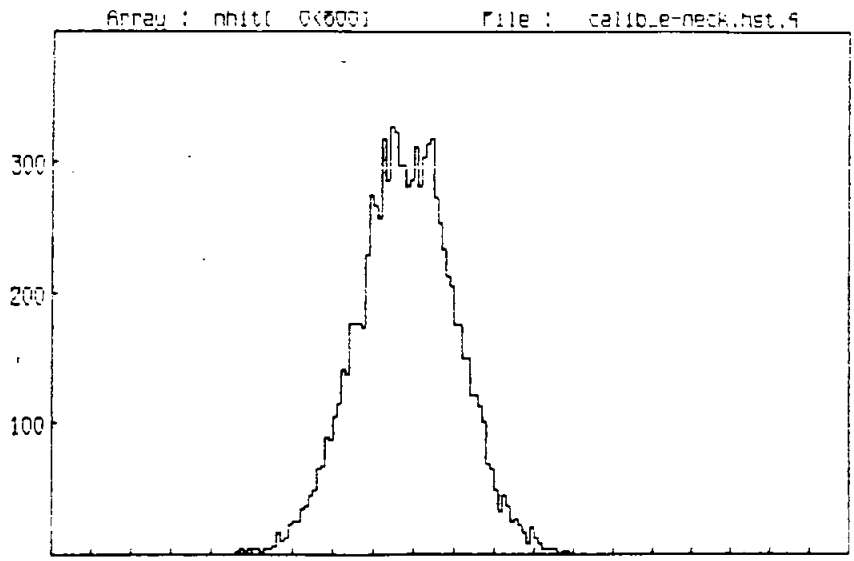
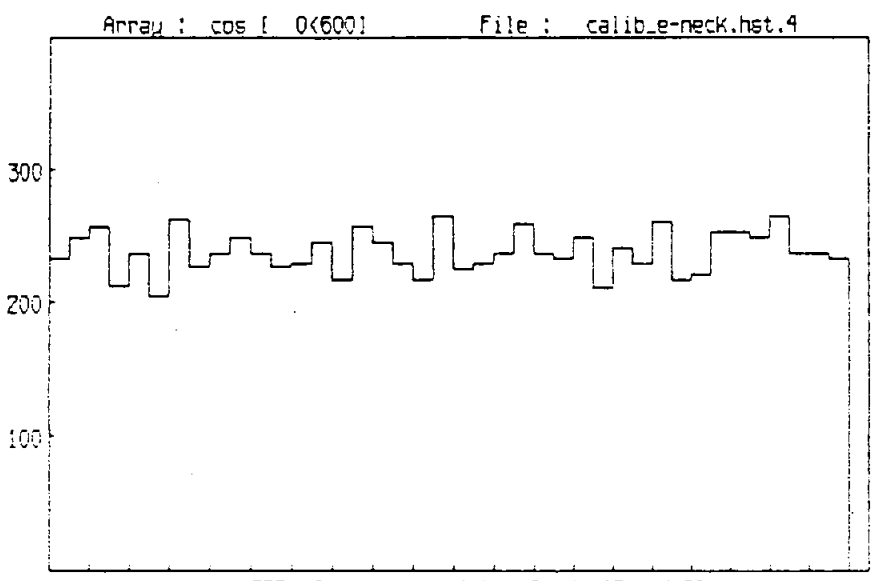


Fig 9



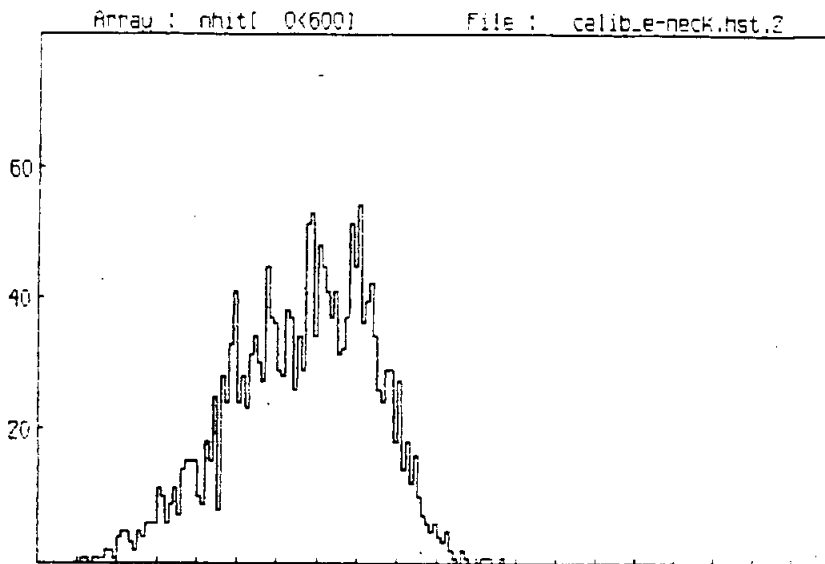
HITx for events with $0 \leq \text{COSx} \leq 40$
 [HIT> 3 PEW> 3 HITW> 3 PEX> 3 HITx> 3]



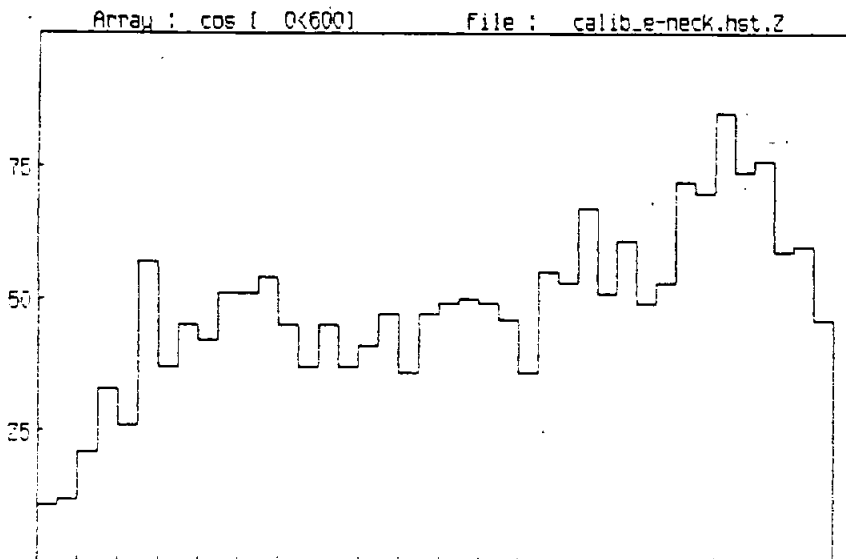
COSx for events with $0 \leq \text{HITx} \leq 199$
 [HIT> 3 PEW> 3 HITW> 3 PEX> 3 HITx> 3]

10,000 e⁻ 10.5 MeV
 non transparent neck and collar
 non transparent neck + collar
 non transparent neck and collar

Fig 10



HITx for events with 0 <= COSx <= 40
 [HIT> 3 PEW> 3 HITW> 3 PEX> 3 HITx> 3]

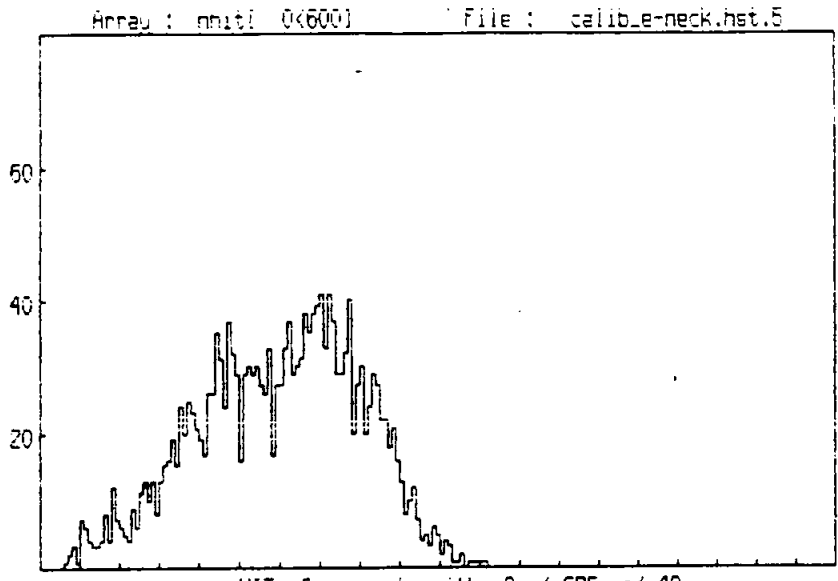


COSx for events with 0 <= HITx <= 199
 [HIT> 3 PEW> 3 HITW> 3 PEX> 3 HITx> 3]

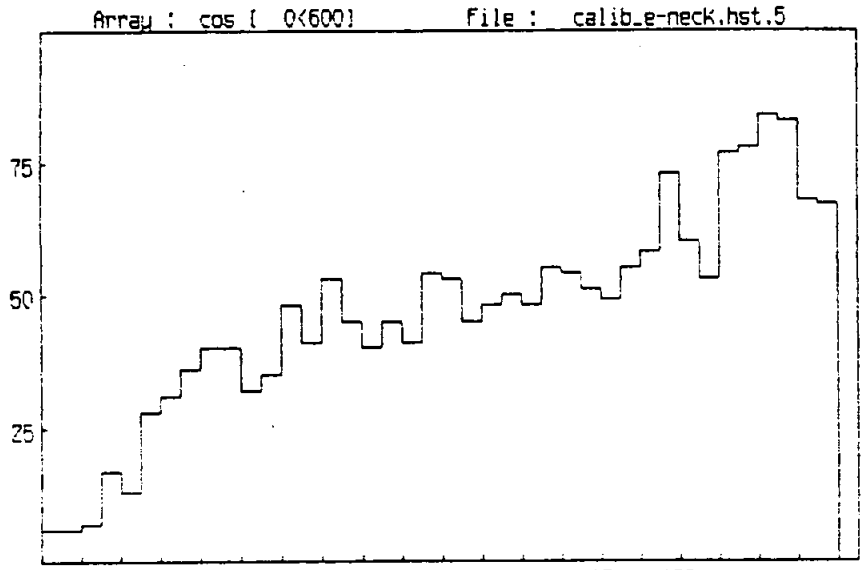
2,000 e⁻ 10.511 MeV

(0, 0, 5520)

more losses from ...
 non-transparent neck



HITx for events with $0 \leq \text{COSx} \leq 40$
 [HIT> 3 PEW> 3 HITW> 3 PEX> 3 HITx> 3]



COSx for events with $0 \leq \text{HITx} \leq 199$
 [HIT> 3 PEW> 3 HITW> 3 PEX> 3 HITx> 3]

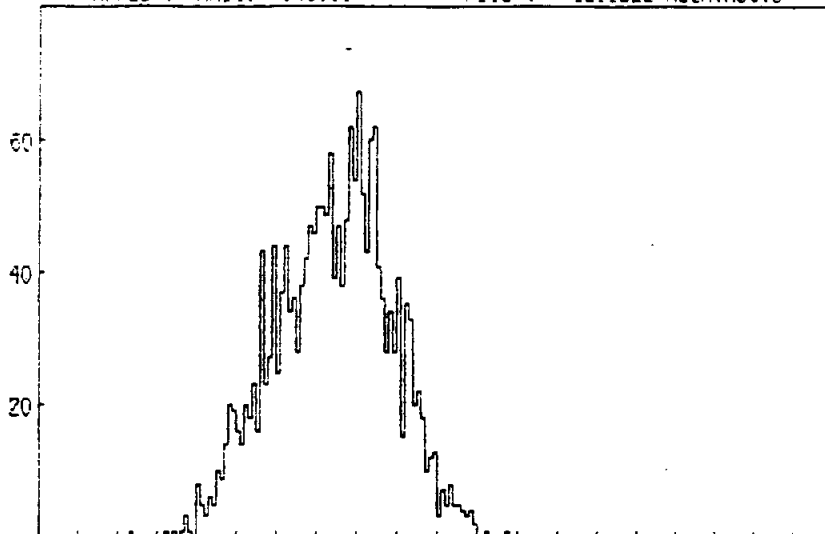
2000 e⁻ 10.5 MeV

(0, 0, 550)

non-transparent neck + collar

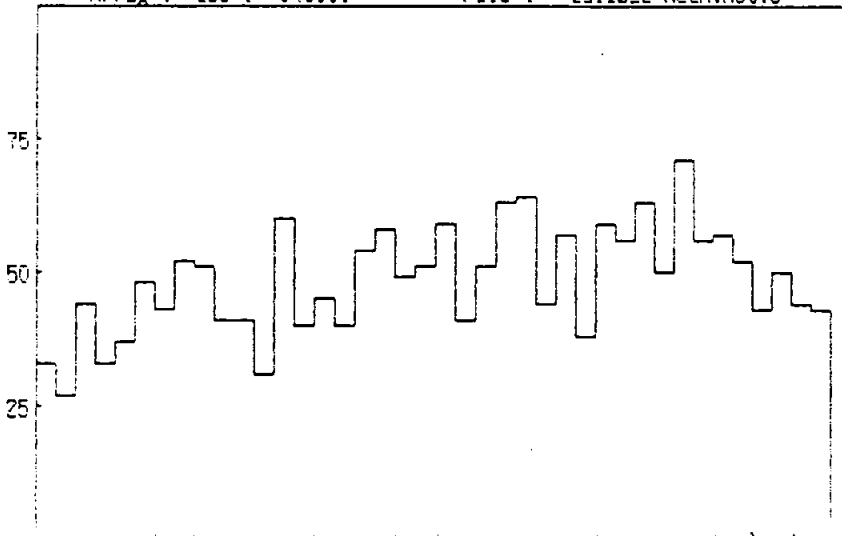
Fig 12

Array : nhit[0(600) File : calib_e-neck.hst.3



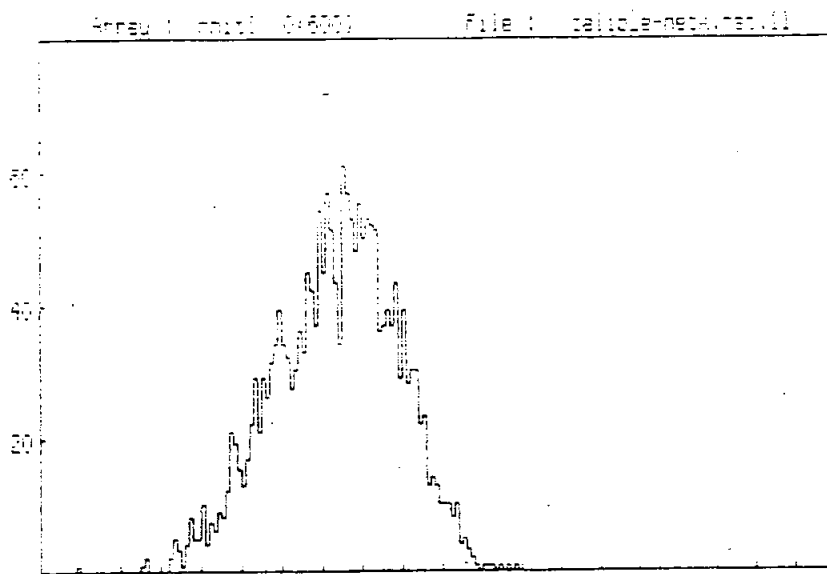
HITx for events with 0 ≤ COSx ≤ 40
(HIT > 3 PEW > 3 HITW > 3 PEX > 3 HITx > 3)

Array : cos [0(600) File : calib_e-neck.hst.3

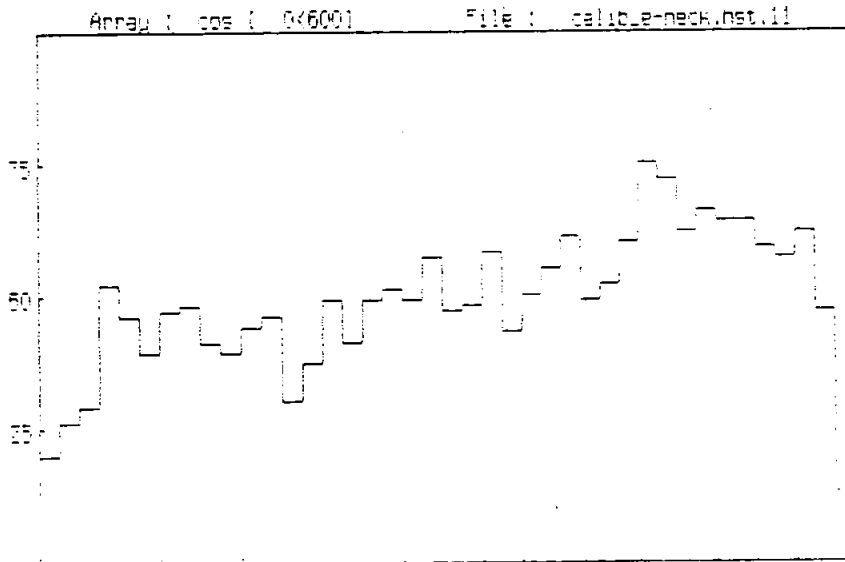


COSx for events with 0 ≤ HITx ≤ 499
(HIT > 3 PEW > 3 HITW > 3 PEX > 3 HITx > 3)

2000 e⁻ 10 S. Ray
 (53.53, 550)
 non transparent neck



H1x for events with 0 <= COSx <= 40
 (H1x 3 PEW 3 HITW 3 PEV 3 HITV 3)

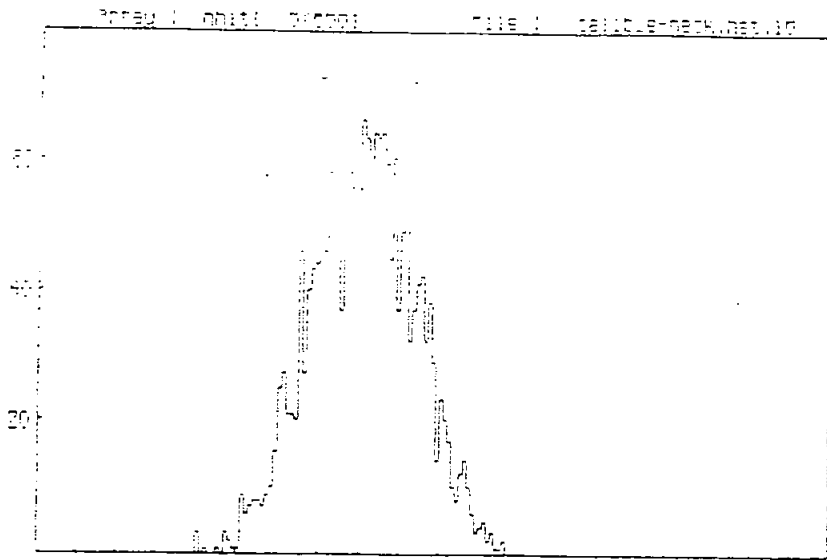


COSx for events with 0 <= H1x <= 185
 (H1x 3 PEW 3 HITW 3 PEV 3 HITV 3)

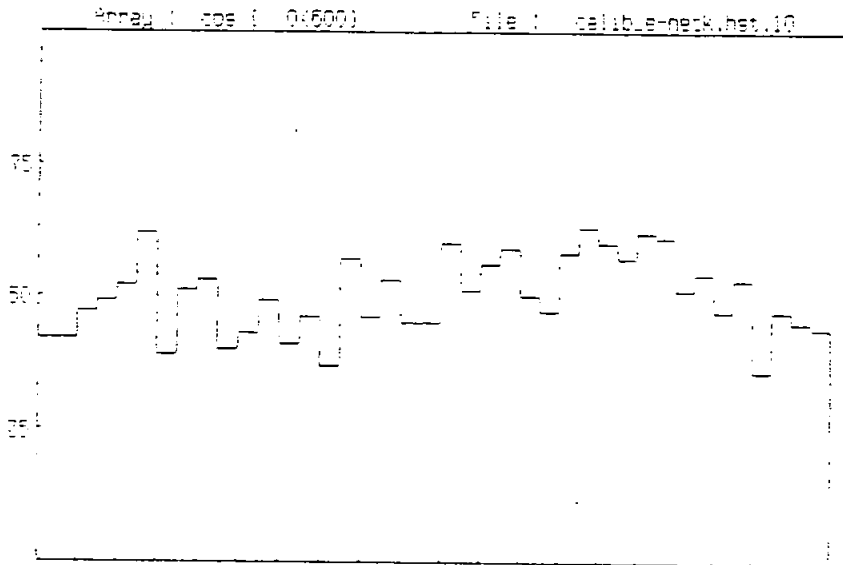
2,000 e⁻ 10.51 MeV

(0.0, 500)

non-transport + neck + collar



nITx for events with $\cos\theta = 40$
 (HITx: 3 PEW: 3 HITW: 3 PEW: 3 HITx: 3)



cosθ for events with $nITx = 133$
 (HITx: 3 PEW: 3 HITW: 3 PEW: 3 HITx: 3)

2,000 e^- 10.5 MeV

(0, 0, 450)

non-transparent neck + collar